Microbiological Research 304 (2026) 128415

Contents lists available at ScienceDirect

Microbiological Research

journal homepage: www.elsevier.com/locate/micres

Disentangling the molecular mechanisms of disease suppression by endophytic *Flavobacterium* sp. 98

Xinya Pan [a,b], Somayah S. Elsayed [b], Gilles P. van Wezel [a,b], Jos M. Raaijmakers [a,b], Víctor J. Carrión [a,b,c,d,*]

[a] Department of Microbial Ecology, Netherlands Institute of Ecology (NIOO-KNAW), Wageningen, Netherlands
[b] Institute of Biology, Leiden University, Leiden, Netherlands
[c] Departamento de Microbiología, Facultad de Ciencias, Universidad de Málaga, Málaga, Spain
[d] Departamento de Protección de Cultivos, Instituto de Hortofruticultura Subtropical y Mediterránea "La Mayora", IHSM-UMA-CSIC, Málaga, Spain

ARTICLE INFO

Keywords:
Flavobacterium
Disease-suppressive soil
Endophytic microbiome
5,6-dimethylbenzimidazole
Molecular mechanisms
Comparative genomics

ABSTRACT

Endophytic microorganisms colonize internal plant tissues and enhance host resistance to pathogens. We previously showed that endophytic *Flavobacterium* sp. 98 (Fl98) protects sugar beet against the fungal root pathogen *Rhizoctonia solani* via biosynthetic gene cluster 298 (BGC298). However, the molecular mechanisms underlying this protection remained poorly understood. Here, comparative metabolomic analyses revealed that knockout of BGC298 led to reduced production of the antifungal compound 5,6-dimethylbenzimidazole (DMB) in Fl98. We hypothesized that BGC298 is involved in regulating DMB biosynthesis and therefore contributes to Fl98's disease suppression as a novel protective mechanism. Subsequent site-directed mutagenesis of the DMB-synthase gene *bluB* abolished DMB production by Fl98, and both ΔBGC298 and Δ*bluB* mutants were compromised in protecting sugar beet seedlings in greenhouse bioassays. Bioinformatic analyses further indicated that *bluB* is widespread across *Flavobacterium*, while BGC298 is limited to a small subset of plant-associated strains. Together, our findings highlight the pivotal role of BGC298 and DMB biosynthesis in plant protection by endophytic *Flavobacterium* sp. 98.

1. Introduction

The plant microbiome plays a crucial role in plant growth and stress resilience by facilitating nutrient uptake and protection against pathogens (Trivedi et al., 2020). Rhizospheric and endophytic microorganisms can suppress plant diseases through various mechanisms including direct antagonism and induced systematic resistance (Gu et al., 2020; Pal et al., 2022; Pieterse et al., 2014; Syed Ab Rahman et al., 2018). Disease-suppressive soils are prominent examples where plants benefit from the associated microorganisms for their protection against pathogen attack (Spooren et al., 2024; Schlatter et al., 2017). In the past decades, extensive studies have been conducted on disease-suppressive soils utilizing both culture- dependent and independent approaches (Carrión et al., 2018; Cordovez et al., 2015; Expósito et al., 2017; Schlatter et al., 2017).

A classic example of disease-suppressive soil is take-all decline, where the reduction of take-all disease was observed in wheat or barley that typically involves *Pseudomonas* species producing selective antimicrobial compounds (Cook, 2003; Mavrodi et al., 2012; Raaijmakers and Weller, 1998; Thomashow et al., 1990). Recent advances in 'omics' technologies have facilitated a more detailed and systematic characterization of the taxonomic and functional diversity of resident microbial communities in soils suppressive to specific root diseases (Cha et al., 2016; Kim et al., 2019; Mendes et al., 2011; Siegel-Hertz et al., 2018). Various bacterial taxa and functions were attributed to the disease suppressive phenomenon. For example, *Chitinophagaceae* and *Flavobacteriaceae* provided protection against fungal infections both in the rhizosphere and root endosphere, presumably via enzymatic degradation of fungal cell walls and production of yet unknown secondary metabolites (Carrión et al., 2019; Yin et al., 2021).

Compared to well-studied protective bacterial taxa such as *Pseudomonas* and *Bacillus* (Dimkić et al., 2022; Van Der Voort et al., 2015; Watrous et al., 2012), the molecular and chemical basis of disease suppression by members of the *Bacteroidetes* phylum remains poorly understood. Our previous study with *Flavobacterium* sp. 98 (Fl98) and *Chitinophaga* sp. 94 (Fl94) identified BGC298 and chitinase as putative

* Corresponding author at: Departamento de Microbiología, Facultad de Ciencias, Universidad de Málaga, Málaga, Spain.
E-mail address: vcarrion@uma.es (V.J. Carrión).

https://doi.org/10.1016/j.micres.2025.128415
Received 13 August 2025; Received in revised form 13 November 2025; Accepted 4 December 2025
Available online 6 December 2025

genetic elements associated with protection of sugar beet seedlings against the fungal root pathogen *Rhizoctonia solani*, respectively (Carrión et al., 2019). BGC298 was enriched in the metagenome of the endosphere of sugar beet seedlings upon *R. solani* attack (Carrión et al., 2019). Transcriptome analyses further revealed that *R. solani* infection upregulated expression levels of BGC298 and chitinase in the sugar beet root endosphere (Carrión et al., 2019). Subsequent bioassays revealed reduced protection of seedlings inoculated with the BGC298 knockout mutant (ΔBGC298) compared to wild type Fl98 (Carrión et al., 2019). Interestingly, homologous genes encoding the PKS module of BGC298 were found exclusively in a small subset of plant-associated *Flavobacterium* genomes. We hypothesized that BGC298 is linked to the biosynthesis of metabolites involved in Fl98's protective effects, and disruption in BGC298 may reduce the production or regulation of these compounds, thereby impairing disease suppression.

To disentangle the mechanisms underlying disease suppression by endophytic *Flavobacterium*, we performed comparative metabolomic analyses and generated additional knockout mutants to elucidate the biosynthesis and function of bioactive compounds produced by Fl98. Our findings revealed novel genes and metabolites contributing to Fl98-mediated plant protection. Among the metabolites downregulated in the ΔBGC298 mutant, we identified 5,6-dimethylbenzimidazole (DMB) as an antifungal compound that inhibits *R. solani* hyphal growth. We validated the biosynthesis of DMB by Fl98 via site-directed mutagenesis of the DMB synthase gene *bluB*. These findings provide new insights into the genetic and metabolic mechanisms underpinning *Flavobacterium*-mediated suppression of *R. solani* and support the potential of endophyte-derived metabolites for microbiome-based crop protection strategies.

2. Materials and methods

2.1. Strains and growth conditions

Wild-type *Flavobacterium* sp. 98 (Fl98) was originally isolated from the root endosphere of sugar beet seedlings grown in *Rhizoctonia*-suppressive soil (Carrión et al., 2019). To investigate the role of the novel NRPS-PKS hybrid cluster BGC298 in Fl98, the PKS module within BGC298 was targeted. A corresponding knockout mutant designated as ΔBGC298 was generated in previous work (Carrión et al., 2019). For this study, bacterial strains were retrieved from glycerol stocks and routinely cultured on 1/10th strength Tryptic Soy Broth (TSB, BD Bacto™) supplemented with 15 g/L agar (BD Bacto™) at 25°C for 2–3 days. *Escherichia coli* strains were grown in lysogeny broth (LB) at 37°C.

The strains and plasmids used in this study are listed in Supplementary Table S1. Antibiotics were used at the following concentrations when necessary: ampicillin (100 μg/mL), erythromycin (100 μg/mL), and rifampicin (50 μg/mL).

2.2. Untargeted metabolomics

2.2.1. Secondary metabolite extraction

Fl98 wildtype and its derived mutants were grown on petri dishes containing 20 mL 1/10th strength Tryptic Soy Broth (TSB, BD Bacto™) supplemented with 15 g/L agar (BD Bacto™) at 25 °C for four days (N = 3 biological replicates). Following incubation, the agar with bacteria lawns was cut into small pieces and submerged in 20 mL of ethyl acetate overnight to extract the metabolites. The ethyl acetate containing the extracted metabolites was then decanted into a clean beaker and allowed to evaporate at room temperature. This extraction process was repeated twice to ensure comprehensive metabolite recovery. The resulting dried extracts were re-dissolved in methanol, passed through PTFE 0.2 μm filters, and transferred to new pre-weighed glass vials. The solvent was removed under a stream of nitrogen until completely dry. The crude extracts were weighed and dissolved in methanol to a final concentration of 1 mg/mL for future LC-MS/MS analysis.

2.2.2. Untargeted LC-MS/MS analysis

LC-MS/MS acquisition was performed using Shimadzu Nexera X2 UHPLC system, coupled to Shimadzu 9030 QTOF mass spectrometer, equipped with a standard ESI source unit, in which a calibrant delivery system (CDS) is installed. Detailed parameters for the measurements can be found in the Supplementary Material.

2.2.3. Data analysis

Raw data obtained from LC-MS analysis were converted to mzXML centroid files using Shimadzu LabSolutions Postrun Analysis. The files were imported into Mzmine 2.53 for data processing with parameters specified in the Supplementary Material (Pluskal et al., 2010). The resulting peak list was uploaded to MetaboAnalyst (Pang et al., 2024) for statistical analysis. Log transformation with pareto scaling was applied to the data. Differences with a twofold change and an FDR-adjusted pvalue < 0.05 were considered statistically significant (unless otherwise stated). Based on these criteria, volcano plots were generated. Analogs and exact matches of the significant features were predicted by using MS2Query (de Jonge et al., 2023).

2.3. Targeted quantification of 5,6-dimethylbenzimidazole

Untargeted metabolomic analysis suggested that 5,6-dimethylbenzimidazole (DMB) was differentially abundant in Fl98 WT and ΔBGC298. This result was further validated via targeted LC-MS. The extracts were prepared as previously and analyzed using the LC-MS/MS (Agilent 1290 LC equipped with an Agilent 6460 C QQQ, Santa Clara, USA). 10 μL of the samples was injected on column (Zorbax Eclipse XDB-C18 column, 2.1 × 150 mm, 3.5 μm, Agilent Santa Clara). The mobile phase included eluent A (milli-Q water with 0.1 % formic acid) and eluent B (acetonitrile with 0.1 % formic acid). The step gradient was set as below: 2 % B for 1 min, increased to 100 % B in 7 min and hold for 3 min. The flow rate was kept at 1 mL/min and the column temperature was set on 35 °C. DMB was detected in positive ionization mode using electrospray. Precursor ion 147.1 *m/z* was used and the product ion 131.2 *m/z* was used for quantification. To confirm the compound the product ions 132.1, 104.2 and 77.2 *m/z* were used as qualifier ions. The data was analyzed in Masshunter 10.0 (Agilent, Santa Clara).

2.4. In vitro activity of DMB

In vitro assays were performed to test the biological activity of standard DMB (Sigma-Aldrich). Pure DMB was dissolved in 100 % methanol and added to 1/5th strength potato dextrose agar (PDA) at varying concentrations (0–500 μg/mL). A 5-mm-diameter plug of *R. solani* mycelium was placed in the middle of each well of 6-well plate and incubated at 25 °C for three days (N = 3 biological replicates). Fungal growth inhibition was monitored by measuring the radial hyphal growth after one, two, and three days of incubation. To check whether the solvent itself had any effect on growth of the fungus, *R. solani* was also exposed to methanol alone.

2.5. Construction of Flavobacterium mutants

2.5.1. Identification of bluB gene

Candidate genes for generating additional knockout mutants of Fl98 in DMB synthase were identified through sequence homology searches. Specifically, BLASTP was used to compare proteins encoded by Fl98 to the query sequence of a known BluB protein involved in DMB biosynthesis as provided below (Campbell et al., 2006). Three genes encoding proteins with high amino acid sequence similarity, namely *98_02485*, *98_06510*, and *98_02510*, were prioritized for subsequent targeted mutagenesis. All three genes encode proteins that contain conserved domains from the Nitroreductase family (Pfam ID: PF00881) and share homology to the query sequence:

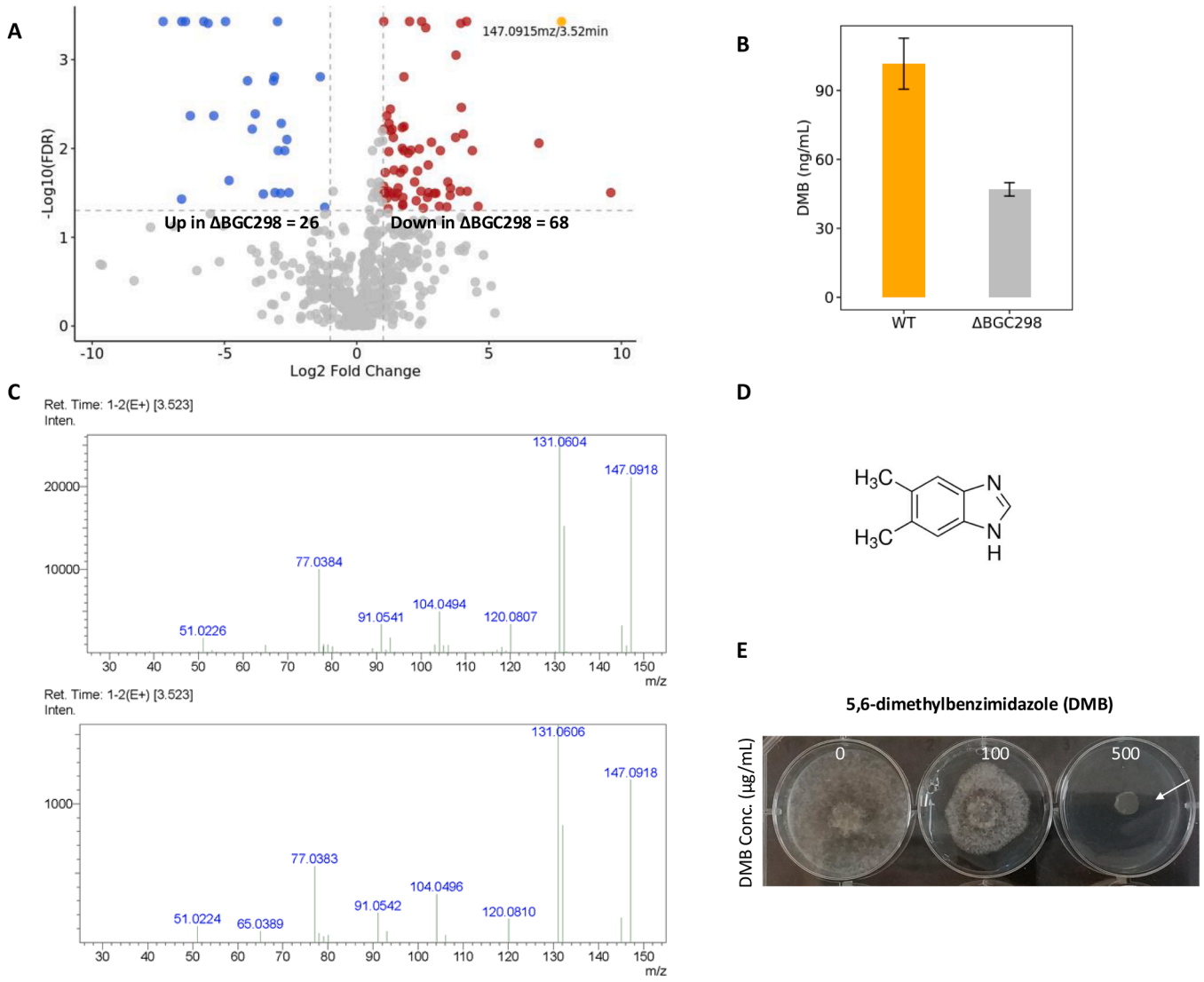

Fig. 1. Identification of the antifungal compound 5,6-dimethylbenzimidazole (DMB) produced by endophytic *Flavobacterium* sp. 98 (Fl98). (**A**) Volcano plot showing differentially abundant metabolites in cell-free culture extracts from Fl98 WT and ΔBGC298 grown on 1/10th TSA. Significant enhancement ('up') and reduction ('down') of mass features in Fl98 mutant ΔBGC298 are represented in blue and red, respectively (fold change > 2, FDR < 0.05). Among the significantly reduced mass features, 5,6 dimethylbenzimidazole (DMB; *m/z* 147.0915, retention time 3.52 min) is highlighted in orange. (**B**) Targeted LC-MS revealed less DMB production by ΔBGC298 compared to WT. (**C**) MS/MS spectra showing identical fragmentation patterns of pure DMB and the corresponding peak in the Fl98 extract. (**D**) Chemical structure of DMB. (**E**) Hyphal growth inhibition of *Rhizoctonia solani* after 5 days of growth on agar medium supplemented with different concentrations of DMB.

MLPDPNGCLTAAGAFSSDERAAVYR-
AIETRRDVRDEFLPEPLSEELIARLLGAAHQAPSVGFMQPWNFVLVRQDE-
TREKVWQAFQRANDEAAEMFSGERQAKYRSLKLE-
GIRKAPLSICVTCDRTRGGAVVLGRTHNPQMDLYSTVCAVQNLWLAAR-
AEGVGVGWVSIFHESEIKAILGIPDHVEIVAWLCLGFVDRLYQEPE-
LAAKGWRQRLPLEDLVFEEGWGVR.

2.5.2. *Site-directed mutagenesis*

To generate *bluB* knockout mutants, the SacB-mediated gene deletion technique was used as described in (Zhu et al., 2017). The list of primers used in this study can be found in Supplementary Table S2. Briefly, 1.5- to 2.5-kb flanking regions upstream and downstream of the target gene were amplified using Phusion DNA polymerase and cloned into the pGemT-easy vector (Promega). The sequence integrity of the cloned fragments was confirmed via Sanger sequencing (Macrogen Europe B. V). Plasmids with verified sequences were digested with restriction enzymes and ligated into the suicide vector pYT313 to construct the final deletion plasmids. Each deletion construct was electroporated into Fl98 following the protocol used by Carrión et al. (2019). Colonies with the plasmid integrated into the genome were selected based on erythromycin resistance. Single erythromycin-resistant colonies were purified on CYE erythromycin plates, and subsequently cultured overnight in CYE broth without erythromycin to facilitate plasmid curing. The cultures were diluted and plated onto CYE agar containing 50 g/L sucrose to select for colonies that had lost the plasmid during a second homologous recombination event. Sucrose-resistant colonies were further purified and screened by PCR to confirm successful gene deletion.

2.6. *In vivo bioassays*

For the bioassays, sugar beet was grown in a field soil conducive to the damping-off disease and inoculated (or not) with *R. solani* AG2–2IIIB, as described previously (Carrión et al., 2019). Briefly, the bacteria were pre-grown on 1/10th strength Tryptone Soy Agar (TSA) and collected in 10 mM $MgSO_4$. Cell suspensions were adjusted to OD600 0.05 and mixed with conducive field soil at an initial density of

A

Gene ID	Alignment (aa)	Identity (%)	E value
98_02485	202	25.743	1.09e-06
98_06510	188	32.979	9.83e-34
98_02510	186	22.043	0.002

*Query = BluB (DMB synthase, UniProt ID: Q92PC8)

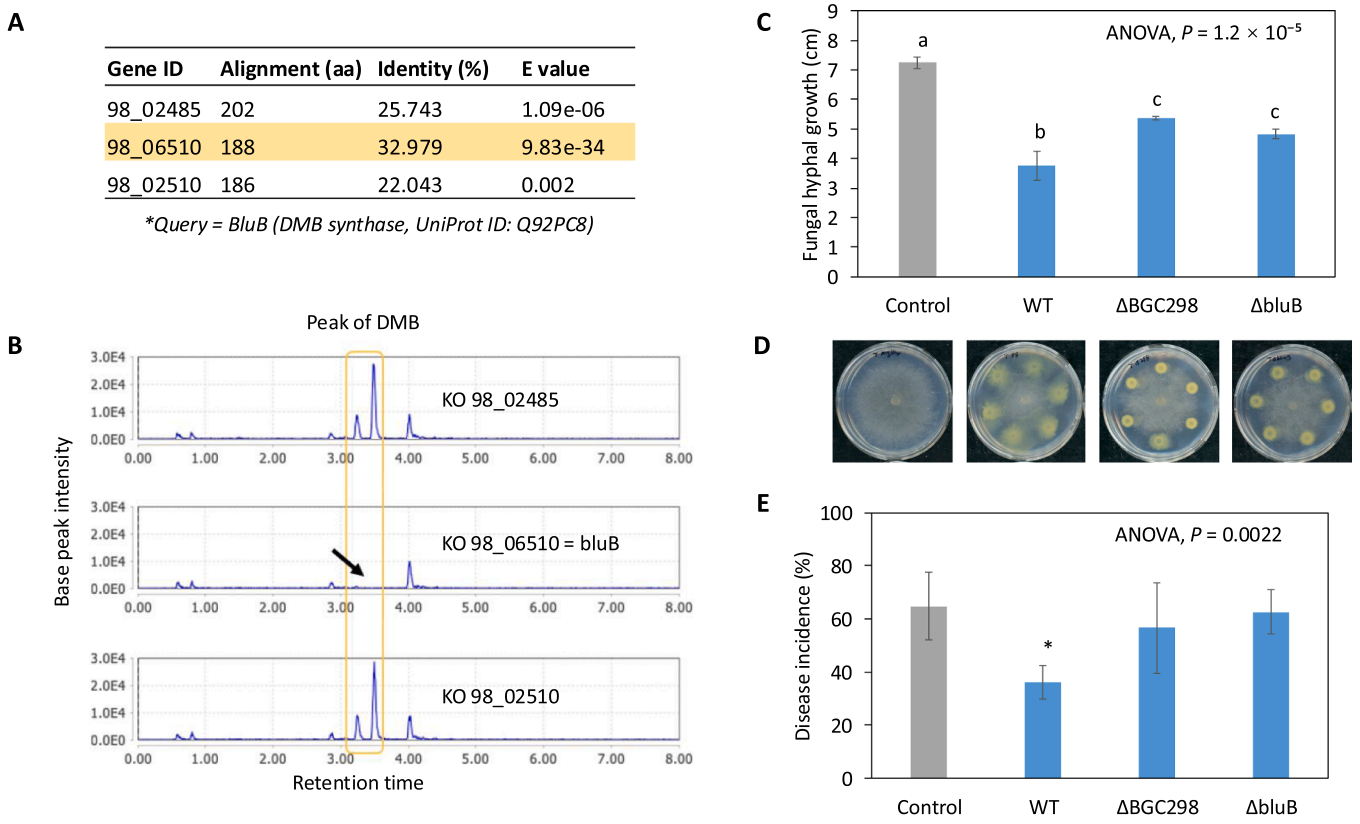

Fig. 2. Validation of *bluB* function in Fl98. (**A**) List of putative DMB synthases (BluB) in Fl98 based on homology search by BLASTP with an experimentally validated *bluB* sequence as query (Campbell et al., 2006). The verified candidate gene of *bluB* in Fl98 is highlighted in yellow. (**B**) Chromatograms indicate the absence of the DMB peak in one of the knock-out (KO) mutants targeting candidate *bluB* genes. (**C**) Bar plot showing the reduced *in vitro* antagonistic activity against *R. solani* by Δ*bluB*. The y axis represents radial hyphal growth of the fungus (inoculated in the center of the plate). Mean values with standard deviations are displayed in the bars. Different letters indicate statistically significant differences between treatments as determined by one-way ANOVA with post hoc Tukey HSD test (N = 3, $P < 0.05$). (**D**) Representative images showing *in vitro* antagonistic activity against hyphal growth of *R. solani* (inoculated in the center) by WT and the mutants (inoculated on the outer edge of the agar plates). (**E**) Disease incidence represents the percentage of sugar beet seedlings with damping-off symptoms (N = 5–8). Asterisks above the bar indicate statistically significant differences compared to the control.

10^7 cells/g soil and approximately 20 % (v/w) soil hydration. Non-inoculated soil was used as a control. Each treatment has eight biological replicates. For each replicate, rectangular trays (19.5 × 6 × 3.5 cm) were filled with 250 g of the conducive soil and 16 sugar beet seeds were sown in a row, 1 cm apart. Those trays were placed in boxes with transparent lids in a growth chamber at 24 °C during the day and 21 °C during the night with a 16 h photoperiod of 180 µmol light m^{-2} s^{-1} at plant level at 70 % relative humidity. After five days, seeds germinated and a single fresh plug (5-mm-diameter) of *R. solani* AG2–2 IIIB previously grown on 1/5th PDA agar was placed approximately 1 cm below the soil surface close to the roots of the first seedling, with the mycelial side toward the plant to allow infection of the first seedling. Spread *of R. solani* through the row of seedlings was scored at regular intervals during two weeks by scoring the number of diseased plants showing the typical damping-off symptoms caused by *R. solani*. For the root colonization assays with Fl98 WT and the *bluB* mutant, rhizosphere and endosphere samples were harvested as described previously (Carrión et al., 2019). Serial dilutions were made and plated on TSA agar dishes with rifampicin and incubated at 25 °C for one week. The amount of CFU per gram of soil and root were determined by colony counting to verify rhizosphere and endosphere colonization, respectively. Statistical test was performed in R to determine significant differences between treatments.

2.7. Statistical analysis

Each experiment was conducted in at least three biological replicates (N = 3). For the metabolomic analysis, statistical tests were performed using MetaboAnalyst (Pang et al., 2024), with correction for multiple comparisons applied using False Discovery Rate (FDR) adjusted *P* values. For the bioassays, statistical tests were performed in R. Differences among treatments were evaluated using one-way ANOVA followed by Tukey's HSD post-hoc test, while pairwise comparisons with the control group were conducted using Dunnett's test.

3. Results and discussion

3.1. Comparative metabolomics reveals reduced DMB production by ΔBGC298

Previous bioassays demonstrated that the ΔBGC298 mutant of Fl98 was less effective in protection of sugar beet against *R. solani* (Carrión et al., 2019). To identify metabolites associated with BGC298, we performed comparative metabolomic analysis of wild-type Fl98 (WT) and ΔBGC298 mutant. Metabolites were extracted from bacterial cultures grown on 1/10th strength Tryptone Soy Agar (TSA). Metabolomic profiling revealed an altered metabolite profile of the ΔBGC298 mutant relative to that of WT Fl98 (PERMANOVA: $R^2 = 0.52176$, $P = 0.1$, Supplementary Figure S1) with a total of 94 mass features that differed

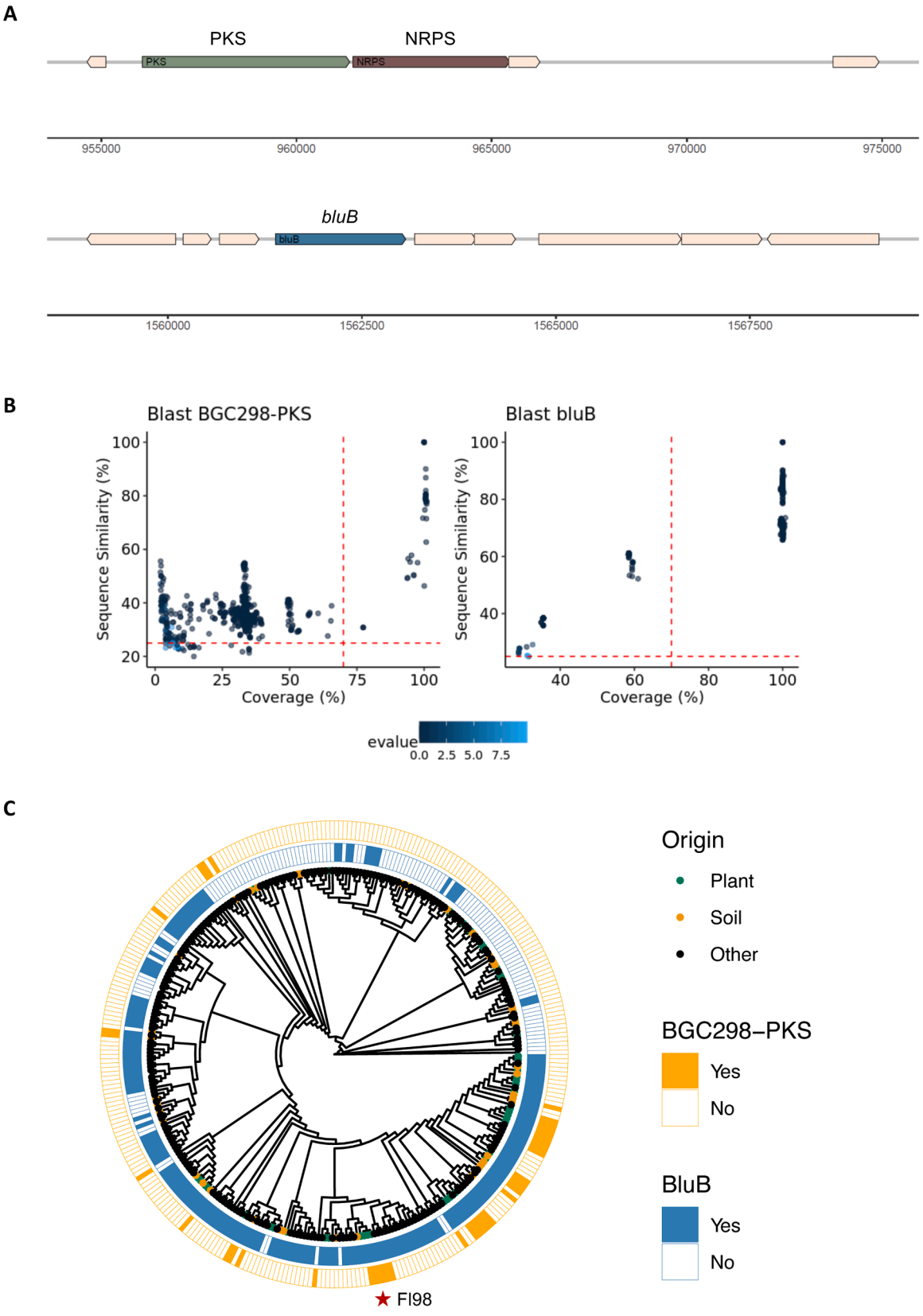

Fig. 3. Distribution of BGC298 and *bluB* in the *Flavobacterium* genus. (**A**) Gene arrangement of BGC298 and *bluB*. BGC298 is composed as a hybrid NRPS-PKS. (**B**) BLASTP results showing the sequence similarity and coverage of *bluB* and BGC298-PKS in the *Flavobacterium* clade. The dash lines represent the cutoffs of 70 % coverage and 25 % sequence similarity. Based on this threshold, *Flavobacterium* genomes with the homologs of *bluB* and BGC298-PKS are highlighted in Fig. 3C. (**C**) Phylogenetic tree of *Flavobacterium* genomes built by phylophlan3 and visualized using ggtree. Tip colors indicate genome origin. For visualization, *F. psychrophilum* and *F. columnare* clades were collapsed to type strains. The inner and outer rings represent the results of searching BluB and the PKS module of BGC298, respectively (BLASTP, coverage > 70 %, sequence similarity > 25 %).

significantly in abundance between WT and ΔBGC298 extracts (Fig. 1A, foldchange > 2, FDR-adjusted $P < 0.05$). Among these metabolites, 26 were significantly enhanced and 68 were reduced in abundance in extracts of ΔBGC298 relative to WT Fl98. Many significant features failed to be annotated with confidence. However, several putative lipid analogs were less abundant in the ΔBGC298 extracts, suggesting possible membrane lipid reprogramming in the mutant that potentially affects cell motility and activity (Supplementary Data S2). Notably, 5,6-dimethylbenzimidazole (DMB) was significantly less abundant in extracts of the ΔBGC298 mutant, which was further verified by targeted liquid chromatography–mass spectrometry (LC–MS) (Fig. 1B). Both DMB peaks from Fl98 extracts and commercial DMB share the same retention time (Supplementary Figure S2). Tandem mass spectrometry (MS/MS) analyses confirmed the identity of DMB produced by Fl98 by showing fragmentation patterns identical to that of the pure DMB standard (Fig. 1C). Interestingly, DMB belongs to benzimidazole derivatives with an azole ring (Fig. 1D), a scaffold known for antimicrobial activity in agricultural and pharmaceutical products (Emami et al., 2022; Price et al., 2015). These findings led to further investigations into the biosynthesis and activity of DMB produced by endophytic Fl98.

3.2. DMB exhibits antifungal activity in a concentration-dependent manner

To assess its potential role in disease suppression, DMB's antifungal activity was evaluated against *R. solani in vitro*. Different concentrations of DMB were tested for their inhibitory effect on hyphal growth of *R. solani*. Addition of DMB to agar medium showed a concentration-dependent inhibition of radial hyphal growth of *R. solani* after 5 days (Fig. 1E). Intriguingly, DMB serves as the lower ligand of vitamin B_{12}, an important cofactor for various prokaryotic enzymes. Many bacteria including *Flavobacterium* species rely on B_{12}-dependent enzymes such as ribonucleotide reductase and methionine synthase to facilitate essential metabolic pathways like DNA replication and repair and amino acid synthesis (Lu et al., 2020; Rodionov et al., 2003). Subsequent genomic analyses, however, revealed that endophytic Fl98 does not harbor the complete B_{12} biosynthetic pathway as described in other prokaryotes (Rodionov et al., 2003); also in our LC-MS/MS analyses, no evidence was found for vitamin B_{12} production by Fl98 (data not shown).

3.3. Genetic basis of DMB biosynthesis in Fl98 and role in disease protection

Previous studies by Campbell et al. (2006) showed that DMB biosynthesis in *Sinorhizobium meliloti* is governed by the DMB synthase gene *bluB*. Bioinformatic analyses of the Fl98 genome identified three candidate genes with some level of homology (22 – 33 %) to *bluB* from *S. meliloti* (Fig. 2A). These three candidate genes were predicted to harbor conserved nitroreductase domains (Pfam ID: PF00881), which are key in DMB biosynthesis. To validate their role in DMB production by Fl98, site-directed knockout mutants were generated for each of these three candidate genes. LC-MS analyses confirmed that DMB was completely absent in mutants disrupted in gene 98_06510; for the other two gene knockouts, no effect on DMB production was observed (Fig. 2B). Knockout mutant 98_06510 is further referred to here as the Δ*bluB* mutant.

Based on the results of the *in vitro* activity of DMB against *R. solani*, we hypothesized that the Δ*bluB* mutant would be compromised in suppressing fungal infection of sugar beet seedlings. Alike ΔBGC298, the Δ*bluB* mutant also showed reduced *in vitro* antagonistic activity against *R. solani* (Figs. 2C, 2D). We then conducted three independent *in planta* bioassays comparing WT Fl98, Δ*bluB* and ΔBGC298 mutants for their ability to protect sugar beet seedlings from *R. solani* root infections. In two of the three assays, however, WT Fl98 failed to provide significant disease protection for yet unknown reasons (data not shown). In the third bioassay, however, WT Fl98 did provide significant disease suppression to a level consistent with the earlier observations (Carrión et al., 2019), whereas the Δ*bluB* and ΔBGC298 mutants failed to protect the sugar beet seedlings from infection (Fig. 2E). While the protective effects of wildtype Fl98 are inconsistent, as observed more often for plant-beneficial bacterial strains (Expósito et al., 2017, 2015), these results indicate that DMB production via *bluB* or regulation via BGC298 is key to the protective effect of endophytic *Flavobacterium* Fl98.

Despite the protective potential of Fl98, the level of disease suppression varied among experiments, reflecting the complexity of interactions operating in soil. The establishment of disease suppression depends on multiple factors, including bacterial colonization efficiency, host plant sensitivity, and interactions with the resident soil microbiome. Subtle shifts in these biotic and abiotic conditions can substantially influence microbial metabolite production and activity in soil and plants, ultimately alternating the suppressive phenotype. Similar inconsistencies *in planta* have been reported with other bacterial strains (Expósito et al., 2017, 2015). Therefore, while Fl98 and DMB biosynthesis contribute to disease suppression, their effects in complex environments likely depend on context-specific ecological and physiological factors that require further investigation.

3.4. Regulation of bluB and BGC298 in endophytic Flavobacterium Fl98

The observations that *bluB* is the key biosynthetic gene for DMB production in Fl98 and that a mutation in BGC298 leads to reduced DMB production (Fig. 1B), suggests that BGC298 regulates DMB biosynthesis in Fl98. Subsequent transcriptome analyses showed that *bluB* expression was not significantly affected in the ΔBGC298 mutant as compared to WT (Supplementary Figure S3). These results indicate that BGC298 does not regulate DMB biosynthesis by affecting *bluB* transcription at sampled timepoints. Interestingly, transcriptomic and RT-qPCR analyses showed that expression of the PKS gene in BGC298 was enhanced upon exposure to root exudates from both healthy and diseased sugar beet seedlings (Supplementary Figure S4), whereas *bluB* expression was upregulated (DESeq2, log2 Fold Change = 0.2009, adjusted $P = 0.0569$ in the stationary phase of Fl98 cultures amended with root exudates from sugar beet seedlings infected with *Rhizoctonia* (Supplementary Figure S4, S5). The subtle changes may reflect insufficient dose and/or suboptimal sampling time for the transcriptional analyses. These findings suggest that expression of *bluB* and of the PKS gene in BGC298 can be triggered by yet unknown constituents of root exudates of *Rhizoctonia*-infected sugar beet seedlings.

Given that *bluB* expression levels were not affected in the BGC298 mutant, we hypothesize that BGC298 may influence DMB production indirectly, potentially through modulation of other metabolites or via post-transcriptional mechanisms, such as protein-level regulation. This suggests that BGC298 could act in a broader regulatory network affecting DMB biosynthesis. Further proteomic and metabolomic analyses will be needed to elucidate the underlying regulatory mechanisms.

3.5. Distribution of bluB and BGC298 in the genus Flavobacterium

Next, we surveyed all *Flavobacterium* genomes available in the NCBI assembly database (N = 504, updated until November 2021) for *bluB* and BGC298. The genomic context of these genes in Fl98 can be found in Fig. 3A. The DMB synthase gene *bluB* appeared conserved and widely distributed within the *Flavobacterium* clade (Figs. 3B, 3C). Although the complete B_{12} biosynthetic pathway is absent in Fl98, the wide distribution of *bluB* suggests a salvage pathway involving DMB biosynthesis in *Flavobacterium* species, which was predominately reported in Proteobacteria and Actinobacteria (Lu et al., 2020). Unlike *bluB*, the core biosynthetic gene of BGC298, encoding the PKS module, is present only in a small subset of the *Flavobacterium* genus (Figs. 3B, 3C). These genomes are closely related to that of the protective root-endophytic strain Fl98 and mostly originated from field soil and plant-associated environments (Fisher's exact test, $P = 2.28 \times 10^{-6}$, OR = 5.99). In addition,

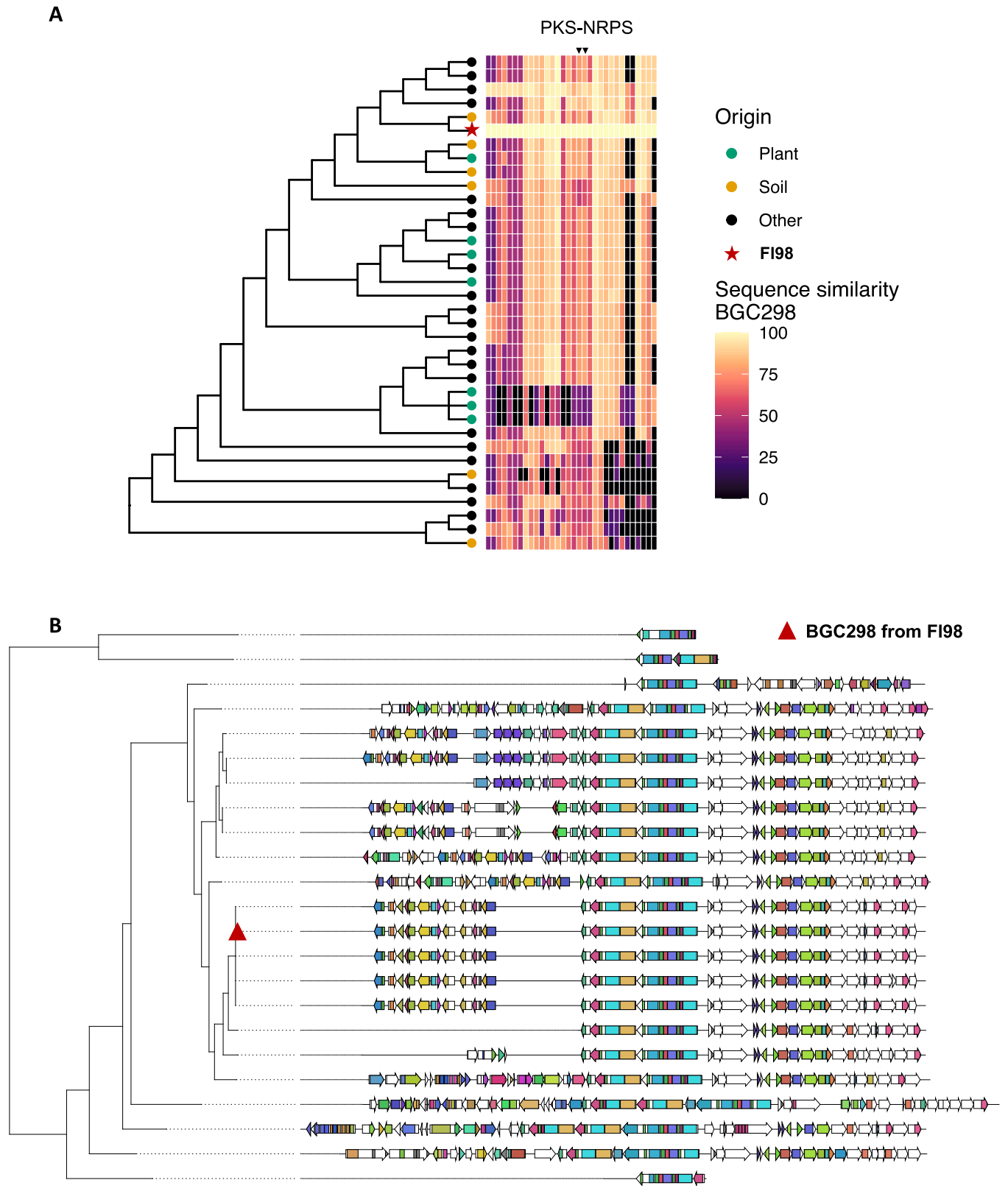

Fig. 4. Evolutionary conservation and diversification of BGC298. (**A**) Subset of the phylogenetic tree of *Flavobacterium* genomes that contain BGC298 homologous genes. Tip colors indicate genome origin. The heatmap depicts similarity differences of genes within BGC298, with core biosynthetic genes encoding PKS and NRPS highlighted. (**B**) Phylogenetic reconstruction of BGC298 and its homologs in other *Flavobacterium* genomes. 23 BGCs with high similarity to BGC298 were detected by BiG-SCAPE (cutoff: 0.7), among a total of 307 PKS-NRPS hybrid BGCs predicted in the 504 *Flavobacterium* genomes from the NCBI assembly database. BGC298 from Fl98 is highlighted.

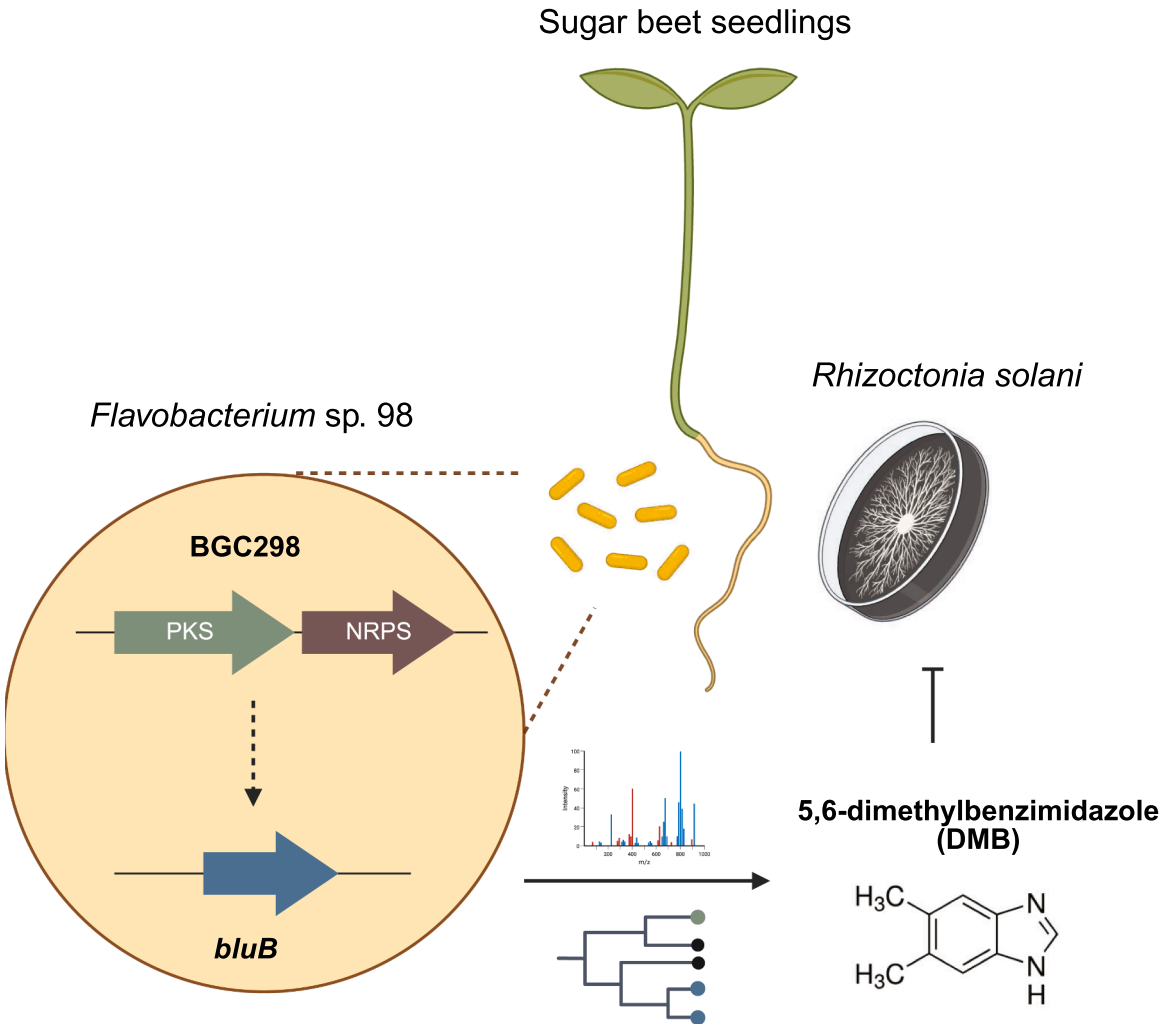

Fig. 5. Conceptual model. *Flavobacterium* sp. 98 (Fl98) provides protection against *Rhizoctonia solani* through BGC298 and *bluB*, which regulate and catalyze the biosynthesis of the antifungal compound 5,6-dimethylbenzimidazole (DMB). While DMB was not detected in the Δ*bluB* mutant, it was less abundant in the ΔBGC298 mutant compared to the wild type. Comparative genomics revealed distinct distribution patterns of these two genes: *bluB* is widespread in the *Flavobacterium* genus, whereas BGC298 occurs only in a limited subset of species with soil and plant associated lifestyles. Together, the function and distribution of these genes suggest specialized adaptive and protective strategies employed by Fl98.

sequence similarity analysis showed both homology and variation among other genes within BGC298 across the 33 *Flavobacterium* genomes encoding the PKS gene (Fig. 4A). Phylogenetic reconstruction of BGC298 and its homologous gene clusters can be found in Fig. 4B. For aquatic *Flavobacterium*, BluB occurs in *F. psychrophilum* but not in *F. columnare*, while BGC298-PKS is absent in both. These results revealed evolutionary conservation and diversification within BGC298, which is potentially linked to yet unknown specialized functional roles in plant-microbe interactions. The distinct distribution patterns of BGC298 and *bluB* suggest that *Flavobacterium* species utilize various genetic strategies for niche adaptation and competitive advantages in diverse ecosystems.

4. Concluding remarks

The *Bacteroidetes* phylum, particularly the *Flavobacterium* genus, has gained increasing attention for its remarkable ability to promote plant growth and suppress plant diseases (Carrión et al., 2019; Kwak et al., 2018; Nishioka et al., 2019; Zheng et al., 2024). *Flavobacterium* members are often enriched in plant-associated environments, especially in response to pathogen attack, yet the molecular mechanisms underlying their protective effects remain largely unknown.

For *Flavobacterium* species, a proposed mechanism to combat plant diseases involves competition or niche exclusion via efficient rhizosphere colonization facilitated by gliding motility and biofilm formation (Magesh et al., 2024; McBride et al., 2009). *Bacteroidetes* are recognized as degraders of polysaccharides and producers of a broad spectrum of enzymes (Lapébie et al., 2019; Pan et al., 2023). For example, *Chitinophaga* species can produce chitinases involved in fungal cell wall degradation and disease suppression (Brabcová et al., 2016; Larsbrink et al., 2017; Lu et al., 2023). Furthermore, secondary metabolite production encoded by biosynthetic gene clusters (BGCs) also plays a key role in the disease suppressive effects of bacteria from the *Bacteroidetes* phylum (Brinkmann et al., 2022; Carrión et al., 2019; Mohr et al., 2015; Silva et al., 2023). Our results suggested that the biosynthesis of antifungal compounds such as DMB and its regulation through BGC298 can contribute to plant protection by Fl98. In addition to DMB, other metabolites including putative fatty acids and terpenoids were also reduced in the ΔBGC298 mutant. Therefore, DMB biosynthesis and regulation represent key but not the only mechanisms underlying BGC298-mediated protective effects.

In this study, we identified novel genes and metabolites, namely *bluB* and DMB, that contribute to disease suppression by *Flavobacterium* (Fig. 5). Comparative metabolomic analyses between the WT and

ΔBGC298 mutant revealed a potential regulatory role of BGC298 in modulating DMB levels in Fl98. Moreover, the contrasting distribution patterns of BGC298 and *bluB* across the *Flavobacterium* genus indicate the evolutionary and ecological heterogeneity of these beneficial bacterial traits. Questions remaining are: which root exudate constituents of infected plant seedlings trigger DMB biosynthesis in Fl98; what is the product of BGC298 and how does BGC298 regulate or impact DMB biosynthesis; does DMB impact directly on plant growth, and are there other metabolites or pathways in Fl98 involved in plant protection? To address these questions, future research should include heterologous expression and overexpression of BGC298, transcriptomic analyses in presence of various environmental triggers in particular plant metabolites present in the plant endosphere (i.e. vasculature) and rhizosphere, investigations into the ecological and functional role of DMB in plant health and in soil microbiome dynamics. Comparative metabolomic analyses of root exudates of healthy and *Rhizoctonia*-infected sugar beet seedlings used in this study did not reveal any putative candidate compounds associated with induction of *bluB* and BGC298 expression. Integrating multi-omics and molecular tools is crucial for developing a system-level model of Bacteroidetes members, such as Fl98, to study their intra- and inter- kingdom interactions. Foundational understanding of their modes of action can guide the development of future agricultural applications to improve soil and plant health.

CRediT authorship contribution statement

Carrion Victor: Writing – review & editing, Writing – original draft, Visualization, Validation, Supervision, Resources, Project administration, Methodology, Investigation, Funding acquisition, Formal analysis, Data curation, Conceptualization. **van Wezel Gilles:** Writing – review & editing, Writing – original draft, Supervision, Resources, Project administration, Methodology, Investigation, Funding acquisition, Formal analysis, Data curation, Conceptualization. **Raaijmakers Jos:** Writing – review & editing, Writing – original draft, Visualization, Validation, Supervision, Resources, Project administration, Methodology, Investigation, Funding acquisition, Formal analysis, Data curation, Conceptualization. **Xinya Pan:** Writing – review & editing, Writing – original draft, Visualization, Validation, Methodology, Investigation, Formal analysis, Data curation, Conceptualization. **Elsayed Somayah:** Writing – review & editing, Writing – original draft, Visualization, Validation, Supervision, Methodology, Investigation, Formal analysis, Data curation, Conceptualization.

Acknowledgments

We thank Hans Zweers and Dr. Lhais Caldas running the LC-MS samples and assisting with the identification of metabolites. We would also like to thank Professor Mark J. McBride for providing the plasmids for *Flavobacterium* transformation. This work is supported by the Netherlands Organization for Scientific Research (NWO) Groot grant OCENW.GROOT.2019.063. V.J.C. and X.P. also receives funding from the Spanish Ministerio de Ciencia, Innovación y Universidades (project RYC2020–029240-I) and Consolidación Investigadora (project CNS2023-145090).

Appendix A. Supporting information

Supplementary data associated with this article can be found in the online version at doi:10.1016/j.micres.2025.128415.

Data availability

Raw LC-MS data has been uploaded to the MassIVE database (submission ID: MSV000098501). Processed metabolomics data comparing Fl98 WT and ΔBGC298 can be found in Supplementary Data S1. MS2Query predictions of the significant features can be found in Supplementary Data S2. The genome sequences are publicly available in the NCBI Assembly database.

References

Brabcová, V., Nováková, M., Davidová, A., Baldrian, P., 2016. Dead fungal mycelium in forest soil represents a decomposition hotspot and a habitat for a specific microbial community. N. Phytol. 210, 1369–1381. https://doi.org/10.1111/NPH.13849.

Brinkmann, S., Kurz, M., Patras, M.A., Hartwig, C., Marner, M., Leis, B., Billion, A., Kleiner, Y., Bauer, A., Toti, L., Pöverlein, C., Hammann, P.E., Vilcinskas, A., Glaeser, J., Spohn, M., Schäberle, T.F., 2022. Genomic and chemical decryption of the bacteroidetes phylum for its potential to biosynthesize natural products. Microbiol. Spectr. 10, e02479-21. https://doi.org/10.1128/spectrum.02479-21.

Campbell, G.R.O., Taga, M.E., Mistry, K., Lloret, J., Anderson, P.J., Roth, J.R., Walker, G. C., 2006. *Sinorhizobium meliloti bluB* is necessary for production of 5,6-dimethylbenzimidazole, the lower ligand of B12. Proc. Natl. Acad. Sci. USA 103, 4634–4639. https://doi.org/10.1073/pnas.0509384103.

Carrión, V.J., Cordovez, V., Tyc, O., Etalo, D.W., de Bruijn, I., de Jager, V.C.L., Medema, M.H., Eberl, L., Raaijmakers, J.M., 2018. Involvement of Burkholderiaceae and sulfurous volatiles in disease-suppressive soils. ISME J. 12, 2307–2321. https://doi.org/10.1038/S41396-018-0186-X.

Carrión, V.J., Perez-Jaramillo, J., Cordovez, V., Tracanna, V., De Hollander, M., Ruiz-Buck, D., Mendes, L.W., van Ijcken, W.F.J., Gomez-Exposito, R., Elsayed, S.S., Mohanraju, P., Arifah, A., van der Oost, J., Paulson, J.N., Mendes, R., van Wezel, G. P., Medema, M.H., Raaijmakers, J.M., 2019. Pathogen-induced activation of disease-suppressive functions in the endophytic root microbiome. Science 366, 606–612. https://doi.org/10.1126/science.aaw9285.

Cha, J.Y., Han, S., Hong, H.J., Cho, H., Kim, D., Kwon, Y., Kwon, S.K., Crusemann, M., Bok Lee, Y., Kim, J.F., Giaever, G., Nislow, C., Moore, B.S., Thomashow, L.S., Weller, D.M., Kwak, Y.S., 2016. Microbial and biochemical basis of a Fusarium wilt-suppressive soil. ISME J. 10, 119–129. https://doi.org/10.1038/ismej.2015.95.

Cook, R.J., 2003. Take-all of wheat. Physiol. Mol. Plant Pathol. 62, 73–86. https://doi.org/10.1016/S0885-5765(03)00042-0.

Cordovez, V., Carrion, V.J., Etalo, D.W., Mumm, R., Zhu, H., van Wezel, G.P., Raaijmakers, J.M., 2015. Diversity and functions of volatile organic compounds produced by *Streptomyces* from a disease-suppressive soil. Front. Microbiol. 6. https://doi.org/10.3389/fmicb.2015.01081.

Dimkić, I., Janakiev, T., Petrović, M., Degrassi, G., Fira, D., 2022. Plant-associated *Bacillus* and *Pseudomonas* antimicrobial activities in plant disease suppression via biological control mechanisms - a review. Physiol. Mol. Plant Pathol. 117, 101754. https://doi.org/10.1016/J.PMPP.2021.101754.

Emami, L., Faghih, Z., Ataollahi, E., Sadeghian, S., Rezaei, Z., Khabnadideh, S., 2022. Azole derivatives: recent advances as potent antibacterial and antifungal agents. Curr. Med. Chem. 30, 220–249. https://doi.org/10.2174/0929867329666220407094430.

Expósito, R.G., de Bruijn, I., Postma, J., Raaijmakers, J.M., 2017. Current insights into the role of rhizosphere bacteria in disease suppressive soils. Front. Microbiol. 8, 2529. https://doi.org/10.3389/fmicb.2017.02529.

Expósito, R.G., Postma, J., Raaijmakers, J.M., De Bruijn, I., 2015. Diversity and activity of *Lysobacter* species from disease suppressive soils. Front. Microbiol. 6, 1243. https://doi.org/10.3389/fmicb.2015.01243.

Gu, S., Wei, Z., Shao, Z., Friman, V.P., Cao, K., Yang, T., Kramer, J., Wang, X., Li, M., Mei, X., Xu, Y., Shen, Q., Kümmerli, R., Jousset, A., 2020. Competition for iron drives phytopathogen control by natural rhizosphere microbiomes, 2020 Nat. Microbiol. 5, 1002–1010. https://doi.org/10.1038/s41564-020-0719-8.

de Jonge, N.F., Louwen, J.J.R., Chekmeneva, E., Camuzeaux, S., Vermeir, F.J., Jansen, R. S., Huber, F., van der Hooft, J.J.J., 2023. MS2Query: reliable and scalable MS2 mass spectra-based analogue search. Nat. Commun. 14, 1752. https://doi.org/10.1038/s41467-023-37446-4.

Kim, D.R., Jeon, C.W., Shin, J.H., Weller, D.M., Thomashow, L., Kwak, Y.S., 2019. Function and distribution of a lantipeptide in strawberry fusarium wilt disease-suppressive soils. Mol. Plant Microbe Interact. 32, 306–312. https://doi.org/10.1094/MPMI-05-18-0129-R.

Kwak, M.J., Kong, H.G., Choi, K., Kwon, S.K., Song, J.Y., Lee, J., Lee, P.A., Choi, S.Y., Seo, M., Lee, H.J., Jung, E.J., Park, H., Roy, N., Kim, H., Lee, M.M., Rubin, E.M., Lee, S.W., Kim, J.F., 2018. Rhizosphere microbiome structure alters to enable wilt resistance in tomato. Nat. Biotechnol. 36, 1100–1109. https://doi.org/10.1038/nbt.4232.

Lapébie, P., Lombard, V., Drula, E., Terrapon, N., Henrissat, B., 2019. Bacteroidetes use thousands of enzyme combinations to break down glycans. Nat. Commun. 10, 1–7. https://doi.org/10.1038/s41467-019-10068-5.

Larsbrink, J., Tuveng, T.R., Pope, P.B., Bulone, V., Eijsink, V.G.H., Brumer, H., McKee, L. S., 2017. Proteomic insights into mannan degradation and protein secretion by the forest floor bacterium *Chitinophaga pinensis*. J. Proteom. 156, 63–74. https://doi.org/10.1016/J.JPROT.2017.01.003.

Lu, X., Heal, K.R., Ingalls, A.E., Doxey, A.C., Neufeld, J.D., 2020. Metagenomic and chemical characterization of soil cobalamin production. ISME J. 14, 53–66. https://doi.org/10.1038/S41396-019-0502-0.

Lu, Z., Kvammen, A., Li, H., Hao, M., Inman, A.R., Bulone, V., McKee, L.S., 2023. A polysaccharide utilization locus from *Chitinophaga pinensis* simultaneously targets chitin and β-glucans found in fungal cell walls. mSphere 8, e00244-23. https://doi.org/10.1128/msphere.00244-23.

Magesh, S., Hurley, A.I., Nepper, J.F., Chevrette, M.G., Schrope, J.H., Li, C., Beebe, D.J., Handelsman, J., 2024. Surface colonization by *Flavobacterium johnsoniae* promotes

its survival in a model microbial community. mBio 15. https://doi.org/10.1128/mbio.03428-23.
Mavrodi, D.V., Mavrodi, O.V., Parejko, J.A., Bonsall, R.F., Kwak, Y.S., Paulitz, T.C., Thomashow, L.S., Weller, D.M., 2012. Accumulation of the antibiotic phenazine-1-carboxylic acid in the rhizosphere of dryland cereals. Appl. Environ. Microbiol. 78, 804–812. https://doi.org/10.1128/AEM.06784-11.
McBride, M.J., Xie, G., Martens, E.C., Lapidus, A., Henrissat, B., Rhodes, R.G., Goltsman, E., Wang, W., Xu, J., Hunnicutt, D.W., Staroscik, A.M., Hoover, T.R., Cheng, Y.Q., Stein, J.L., 2009. Novel features of the polysaccharide-digesting gliding bacterium *Flavobacterium johnsoniae* as revealed by genome sequence analysis. Appl. Environ. Microbiol. 75, 6864–6875. https://doi.org/10.1128/AEM.01495-09.
Mendes, R., Kruijt, M., De Bruijn, I., Dekkers, E., Van Der Voort, M., Schneider, J.H.M., Piceno, Y.M., DeSantis, T.Z., Andersen, G.L., Bakker, P.A.H.M., Raaijmakers, J.M., 2011. Deciphering the rhizosphere microbiome for disease-suppressive bacteria. Science 332, 1097–1100. https://doi.org/10.1126/science.1203980.
Mohr, K.I., Volz, C., Jansen, R., Wray, V., Hoffmann, J., Bernecker, S., Wink, J., Gerth, K., Stadler, M., Müller, R., 2015. Pinensins: the first antifungal lantibiotics. Angew. Chem. Int. Ed. 54, 11254–11258. https://doi.org/10.1002/anie.201500927.
Nishioka, T., Marian, M., Kobayashi, I., Kobayashi, Y., Yamamoto, K., Tamaki, H., Suga, H., Shimizu, M., 2019. Microbial basis of Fusarium wilt suppression by *Allium* cultivation. Sci. Rep. 9, 1–9. https://doi.org/10.1038/s41598-018-37559-7.
Pal, G., Saxena, S., Kumar, K., Verma, A., Sahu, P.K., Pandey, A., White, J.F., Verma, S.K., 2022. Endophytic *Burkholderia*: multifunctional roles in plant growth promotion and stress tolerance. Microbiol. Res. 265, 127201. https://doi.org/10.1016/J.MICRES.2022.127201.
Pan, X., Raaijmakers, J.M., Carrión, V.J., 2023. Importance of Bacteroidetes in host–microbe interactions and ecosystem functioning. Trends Microbiol. 31, 959–971. https://doi.org/10.1016/J.TIM.2023.03.018.
Pang, Z., Lu, Y., Zhou, G., Hui, F., Xu, L., Viau, C., Spigelman, A.F., Macdonald, P.E., Wishart, D.S., Li, S., Xia, J., 2024. MetaboAnalyst 6.0: towards a unified platform for metabolomics data processing, analysis and interpretation. Nucleic Acids Res. 52, W398–W406. https://doi.org/10.1093/NAR/GKAE253.
Pieterse, C.M.J., Zamioudis, C., Berendsen, R.L., Weller, D.M., Van Wees, S.C.M., Bakker, P.A.H.M., 2014. Induced systemic resistance by beneficial microbes. Annu. Rev. Phytopathol. 52, 347–375. https://doi.org/10.1146/annurev-phyto-082712-102340.
Pluskal, T., Castillo, S., Villar-Briones, A., Orešič, M., 2010. MZmine 2: modular framework for processing, visualizing, and analyzing mass spectrometry-based molecular profile data. BMC Bioinform. 11, 1–11. https://doi.org/10.1186/1471-2105-11-395.
Price, C.L., Parker, J.E., Warrilow, A.G., Kelly, D.E., Kelly, S.L., 2015. Azole fungicides – understanding resistance mechanisms in agricultural fungal pathogens. Pest Manag. Sci. 71, 1054–1058. https://doi.org/10.1002/PS.4029.
Raaijmakers, J.M., Weller, D.M., 1998. Natural plant protection by 2,4-diacetylphloroglucinol-producing *Pseudomonas* spp. in Take-all decline soils. Mol. Plant Microbe Interact. 11, 144–152. https://doi.org/10.1094/MPMI.1998.11.2.144.
Rodionov, D.A., Vitreschak, A.G., Mironov, A.A., Gelfand, M.S., 2003. Comparative genomics of the vitamin B12 metabolism and regulation in prokaryotes. J. Biol. Chem. 278, 41148–41159. https://doi.org/10.1074/jbc.M305837200.
Schlatter, D., Kinkel, L., Thomashow, L., Weller, D., Paulitz, T., 2017. Disease suppressive soils: new insights from the soil microbiome. Phytopathology 107, 1284–1297. https://doi.org/10.1094/PHYTO-03-17-0111-RVW.
Siegel-Hertz, K., Edel-Hermann, V., Chapelle, E., Terrat, S., Raaijmakers, J.M., Steinberg, C., 2018. Comparative microbiome analysis of a Fusarium wilt suppressive soil and a Fusarium wilt conducive soil from the Châteaurenard region. Front. Microbiol. 9, 568. https://doi.org/10.3389/FMICB.2018.00568.
Silva, S.G., Nabhan Homsi, M., Keller-Costa, T., Rocha, U., Costa, R., 2023. Natural product biosynthetic potential reflects macroevolutionary diversification within a widely distributed bacterial taxon. mSystems 8, e00643-23. https://doi.org/10.1128/msystems.00643-23.
Spooren, J., van Bentum, S., Thomashow, L.S., Pieterse, C.M.J., Weller, D.M., Berendsen, R.L., 2024. Plant-driven assembly of disease-suppressive soil microbiomes. Annu. Rev. Phytopathol. 62, 1–30. https://doi.org/10.1146/annurev-phyto-021622-100127.
Syed Ab Rahman, S.F., Singh, E., Pieterse, C.M.J., Schenk, P.M., 2018. Emerging microbial biocontrol strategies for plant pathogens. Plant Sci. 267, 102–111. https://doi.org/10.1016/J.PLANTSCI.2017.11.012.
Thomashow, L.S., Weller, D.M., Bonsall, R.F., Pierson, L.S., 1990. Production of the antibiotic phenazine-1-carboxylic acid by fluorescent *Pseudomonas* species in the rhizosphere of wheat. Appl. Environ. Microbiol. 56, 908–912. https://doi.org/10.1128/aem.56.4.908-912.1990.
Trivedi, P., Leach, J.E., Tringe, S.G., Sa, T., Singh, B.K., 2020. Plant–microbiome interactions: from community assembly to plant health. Nat. Rev. Microbiol. 18, 607–621. https://doi.org/10.1038/s41579-020-0412-1.
Van Der Voort, M., Meijer, H.J.G., Schmidt, Y., Watrous, J., Dekkers, E., Mendes, R., Dorrestein, P.C., Gross, H., Raaijmakers, J.M., 2015. Genome mining and metabolic profiling of the rhizosphere bacterium *Pseudomonas* sp. SH-C52 for antimicrobial compounds. Front. Microbiol. 6, 693. https://doi.org/10.3389/fmicb.2015.00693.
Watrous, J., Roach, P., Alexandrov, T., Heath, B.S., Yang, J.Y., Kersten, R.D., Van Der Voort, M., Pogliano, K., Gross, H., Raaijmakers, J.M., Moore, B.S., Laskin, J., Bandeira, N., Dorrestein, P.C., 2012. Mass spectral molecular networking of living microbial colonies. Proc. Natl. Acad. Sci. USA 109, E1743–E1752. https://doi.org/10.1073/pnas.1203689109.
Yin, C., Casa Vargas, J.M., Schlatter, D.C., Hagerty, C.H., Hulbert, S.H., Paulitz, T.C., 2021. Rhizosphere community selection reveals bacteria associated with reduced root disease. Microbiome 9, 1–18. https://doi.org/10.1186/s40168-020-00997-5.
Zheng, W., Wang, N., Qian, G., Qian, X., Liu, W., Huang, L., 2024. Cross-niche protection of kiwi plant against above-ground canker disease by beneficial rhizosphere *Flavobacterium*. Commun. Biol. 7, 1–10. https://doi.org/10.1038/s42003-024-07208-z.
Zhu, Y., Thomas, F., Larocque, R., Li, N., Duffieux, D., Cladière, L., Souchaud, F., Michel, G., McBride, M.J., 2017. Genetic analyses unravel the crucial role of a horizontally acquired alginate lyase for brown algal biomass degradation by *Zobellia galactanivorans*. Environ. Microbiol. 19, 2164–2181. https://doi.org/10.1111/1462-2920.13699.